Acta Crystallographica Section D
Biological Crystallography
ISSN 0907-4449

Crystallization of an AMPA receptor binding domain without agonist: importance of carbohydrate content and flash-cooling conditions

James Féthière,[a]† Arnold Andersson,[a]‡ Kari Keinänen[b] and Dean R. Madden[a]*

[a]Ion Channel Structure Research Group, Max Planck Institute for Medical Research, Jahnstrasse 29, 69120 Heidelberg, Germany, and [b]Viikki Biocenter, Department of Biosciences (Division of Biochemistry) and Institute of Biotechnology, PO Box 56, FIN-00014 University of Helsinki, Finland

† Present address: m-phasys, Vor dem Kreuzberg 17, 72070 Tübingen, Germany.
‡ Present address: WM-data eSolutions, Axel Johanssons gata 4-6, 75451 Uppsala, Sweden.

Correspondence e-mail: madden@mpimf-heidelberg.mpg.de

Received 5 June 2000
Accepted 9 October 2000

An AMPA-specific ionotropic glutamate receptor binding domain was overexpressed using the baculovirus system and purified by immunoaffinity and metal-affinity chromatography. Purified protein was enzymatically deglycosylated. Both glycosylated and deglycosylated proteins crystallized under the same conditions and in the same space group (*P*2). In both cases, it was observed that the use of MPD as a cryoprotectant induced a significant reduction in the unit-cell volume compared with glycerol or sucrose. For crystals of deglycosylated protein, cryoprotection with MPD also yielded a dramatic improvement in resolution.

1. Introduction

Glutamate is the major excitatory neurotransmitter in the central nervous system. It interacts with specific ionotropic receptors in the post-synaptic membrane that are thought to play a central role in the regulation of synaptic strength, in learning processes and in a number of neuropathologies (Dingledine *et al.*, 1999; Hollmann & Heinemann, 1994; Brennan, 1994). These glutamate receptors (GluR) form oligomeric ligand-gated ion channels containing four or possibly five subunits of approximately 50–165 kDa each (Hollmann & Heinemann, 1994; Nakanishi & Masu, 1994). They have been sub-classified according to their pharmacological specificity for different agonists, one of which is α-amino-3-hydroxy-5-methyl-4-isoxazolepropionate (AMPA). Like other ligand-gated ion channels, some GluRs exhibit desensitization: following activation, the channel closes despite the continuing presence of certain agonists (Hollmann & Heinemann, 1994; Nakanishi & Masu, 1994).

The glutamate-binding domain (S1S2) is formed by two extracellular sequences (S1 and S2) and its core exhibits weak sequence homology to the prokaryotic periplasmic binding proteins (PBPs; Kuusinen *et al.*, 1995; Nakanishi *et al.*, 1990; Stern-Bach *et al.*, 1994). Recently, the crystal structure of the core ligand-binding domain of the AMPA-receptor subunit GluR-B was solved in complex with the apparently non-desensitizing agonist kainate (Armstrong *et al.*, 1998). It confirmed the structural similarity to the PBP and located the agonist-binding site in a cleft formed between two lobes or subdomains of the protein. However, several fundamental questions remain, including the nature of the conformational changes associated with ligand binding and how the S1S2 core domain is linked to the membrane-associated domains that form the pore. We have obtained crystals of the GluR-B S1S2 binding domain in the absence of ligand. The crystallized construct includes functionally important peptides omitted from the core domain (Armstrong *et al.*, 1998); these peptides

represent approximately 15% of the total mass of the S1S2 binding domain, modulate channel-desensitization properties (Sommer *et al.*, 1990; Villarroel *et al.*, 1998; Krupp *et al.*, 1998) and link the core domain to the membrane-associated domains in the intact receptor. Comparison of this ligand-free structure with the kainate-bound core should help to clarify the mechanism by which ligand binding is coupled to channel opening and/or desensitization.

2. Methods and results

2.1. Expression and purification

The full-length S1S2 binding module of the AMPA-specific GluR-B subunit (S1S2-B) comprises residues 382–523 (S1; GluR-B mature sequence numbering) joined directly to residues 627–791 (S2), with an N-terminal FLAG epitope and a C-terminal hexahistidine tag (Kuusinen *et al.*, in preparation). The protein was expressed in an insect cell system and purified essentially as described by Madden *et al.* (2000). The second purification step involved metal-affinity instead of ion-exchange chromatography, yielding highly pure protein (Fig. 1). Typically, 10–20 mg of pure material was obtained from 15–30 l. Final protein concentration (to 5 mg ml^{-1}) and buffer exchange (25 m*M* NaCl, 20 m*M* Tris–HCl pH 7.5) were performed in a Centriprep-10 concentrator. As determined by fluorescence titration measurements (Abele *et al.*, 2000), the material bound AMPA with an equilibrium dissociation constant of 27 n*M*, similar to values observed for the intact membrane-bound receptor (Keinänen *et al.*, 1994).

2.2. Crystallization of native S1S2-B

Initial conditions for crystallization of the glycosylated S1S2-B protein were identified using a sparse-matrix screen (Jancarik & Kim, 1991); most included polyethylene glycol (PEG) as the precipitant. Microscopic needles and plates appeared together with heavy precipitate within a day. Better control of nucleation and reduced precipitation were obtained by refinement of conditions, in particular by the inclusion of L-arginine in the crystallization drop. S1S2-B was crystallized at 289 K using the hanging-drop method. The reservoir contained 500 µl of 18–21% PEG 3350, 0.1 *M* Tris pH 8.0, 0.3 *M* Li_2SO_4 and 5 m*M* L-arginine. Drops contained 5 µl of reservoir solution mixed with 5 µl of protein stock solution (5 mg ml^{-1}). Plate-shaped crystals appeared within 3 d and grew to maximum dimensions of 150 × 150 × 50 µm.

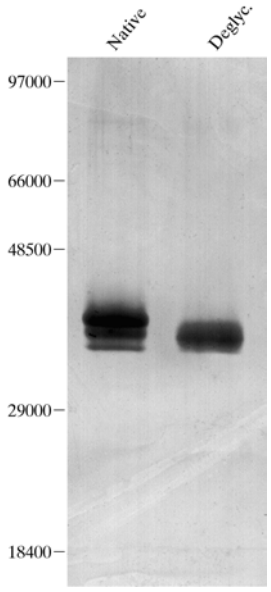

Figure 1
SDS–PAGE gel showing the deglycosylation of recombinant S1S2-B. Native, native recombinant S1S2-B secreted from the insect cells showing the triplet band; Deglyc., enzymatically deglycosylated S1S2-B.

2.3. Initial data collection

Diffraction from crystals of native S1S2-B could not be recorded using a laboratory X-ray source at either room temperature or 100 K, and these crystals showed no diffraction at room temperature using synchrotron radiation. However, when cryoprotected with 25% glycerol or sucrose and flash-cooled in liquid nitrogen, diffraction was observed at ID14-3 (ESRF) at 100 K. The resolution was very variable. Some crystals showed diffraction to the water ring, but these always exhibited badly split multiple lattices. Nevertheless, they indicated the potential for high-resolution diffraction. Single-crystal data sets were obtained to 7–8 Å resolution. For all crystals that could be indexed, analysis by *XDS* of the lattice geometry (Kabsch, 1988) suggested that the space group might be *P*2; for many crystals, the lattice geometry would also have been consistent with the higher symmetry groups *C*2 or *C*222. In these cases, the data were scaled and merged in each of the three candidate space groups: $R_{\rm merge}$ values were consistent only with space group *P*2 ($a \simeq 87$, $b \simeq 87$, $c \simeq 233$ Å, $\beta \simeq 100^\circ$). The intensity distribution of the integrated reflections analyzed by *TRUNCATE* (French & Wilson, 1978; Collaborative Computational Project, Number 4, 1994; Rees, 1980) suggested the presence of merohedral twinning. Twinning is possible in space group *P*2 only in the case of fortuitous unit-cell geometry (Yeates & Fam, 1999), a condition fulfilled by the pseudo-centered geometry of our lattice ($|\overline{c}|\cos\beta \simeq -|\overline{a}|/2$), as detected by *XDS*. The twinning operator was located in the *P*2 *ac* plane, *i.e.* perpendicular to the true crystallographic twofold axis.

In an attempt to improve the crystal quality, alternative cryoprotection protocols were investigated. Cryoprotection with 10% MPD (2-methyl-2,4-pentanediol) with omission of Li_2SO_4 from the soaking buffer provided roughly equivalent diffraction to that seen with 25% glycerol or sucrose (Fig. 2). However, the long *c* axis was reduced by as much as 20% to 186 Å, breaking the pseudo-centering of the lattice geometry and thus facilitating definitive space-group identification.

2.4. Enzymatic deglycosylation

In another attempt to improve diffraction quality, the protein was deglycosylated before crystallization. S1S2-B eluted from the Ni^{2+} column migrated as a triplet on SDS–PAGE (Fig. 1). The fastest (and faintest) of these bands had

the electrophoretic mobility expected from the amino-acid sequence. However, the two higher molecular-weight bands were more intense and probably represent different isoforms of S1S2-B resulting from incomplete or heterogeneous glycosylation at its two N-terminal N-glycosylation sites. Lepidopteran cells exhibit considerable heterogeneity in the glycosylation of recombinant proteins (Davidson *et al.*, 1990; Kulakosky *et al.*, 1998); in particular, the incorporation of complex-type carbohydrates depends on the time of infection (Davidson & Castellino, 1991). S1S2-B was harvested 90–96 h post-infection, a time at which the activation of complex-type processing glycosyltransferases may have been triggered. This chemical heterogeneity and the intrinsic conformational flexibility of carbohydrates are generally considered to be detrimental for crystallization (Wyss & Wagner, 1996), and in several cases enzymatic deglycosylation has proven critical for obtaining well diffracting crystals, *e.g.* human lactoferrin, soluble binding domain of human IL10-R1, *Aspergillus ficuum* phytase and T-cell glycoprotein CD2 (Baker *et al.*, 1994; Hoover *et al.*, 1999; Grueninger-Leitch *et al.*, 1996; Davis *et al.*, 1993).

Partial enzymatic deglycosylation was performed with a mixture of neuraminidase and endo-F2 in a sodium acetate buffer (pH 5.0) for 24 h at 277 K at enzyme:protein ratios of 1:2500 and 1:700, respectively. This resulted in a single band having a molecular weight close to the low molecular weight band in the untreated preparation (Fig. 1). Based on the specificities of the enzymes used, chemical deglycosylation should have removed any bi-antennary complex-type oligosaccharides from the protein, leaving only single *N*-acetylglucosamine moieties. The partially deglycosylated protein was separated from the glycosidases on a Ni^{2+} column prior to crystallization and yielded a single band by isoelectric focusing gel electrophoresis (data not shown). The binding affinity for glutamate, kainate and AMPA was not affected by the presence or absence of carbohydrate moieties on S1S2-B (Kuusinen *et al.*, in preparation). EndoH had no effect on the mobility of the S1S2-B triplet, suggesting that the oligosaccharides are of the bi-antennary complex type (data not shown). Deglycosylated S1S2-B crystallized under the same conditions and with the same morphology as native S1S2-B. S1S2-B expressed in the presence of tunicamycin and, therefore, completely lacking glycosylation does not crystallize under the same conditions or in the same morphology. However, under slightly different conditions, small crystals are obtained that have a different morphology; so far these crystals have not exhibited high-resolution diffraction.

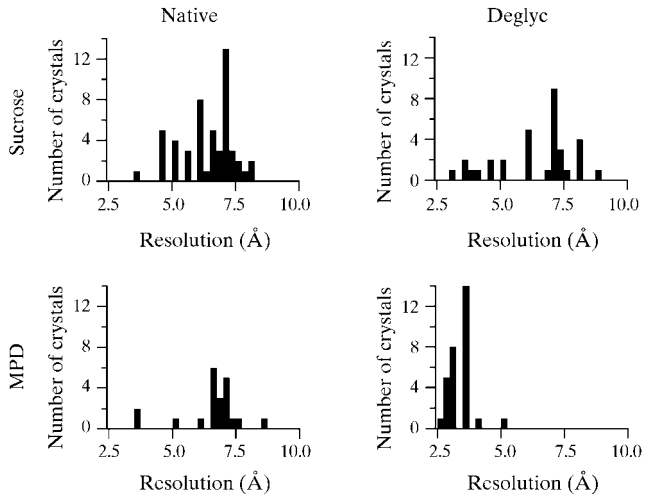

Figure 2
Histograms of the diffraction limits observed with S1S2-B crystals from native and deglycosylated protein cryoprotected with sucrose or MPD (binning width, 0.25 Å).

2.5. High-resolution diffraction requires deglycosylation and shrinkage

When cryoprotected with sucrose or glycerol, crystals of partially deglycosylated S1S2-B showed only a marginal improvement in diffraction quality compared with crystals of glycosylated protein (Fig. 2). However, they exhibited a dramatic improvement in resolution when flash-cooled in MPD. As had been seen with crystals of the glycosylated protein, flash-cooling in MPD also caused shrinkage of the *c* axis. Since neither glycerol nor sucrose cause an equivalent unit-cell change, the shrinkage appears to reflect the influence of MPD on the lattice, consistent with the observation that crystals deteriorate rapidly when soaked in MPD at room temperature. Such shrinkage of the unit cell accompanied by an increase in resolution is not uncommon upon flash-cooling of crystals (Mitchell & Garman, 1994; Schick & Jurnak, 1994). Recently, a controlled shrinkage protocol proved critical to the structure determination of the yeast RNA polymerase II (Cramer *et al.*, 2000). However, in our case, shrinkage provided much better and more uniformly diffracting crystals only when combined with the partial deglycosylation of the protein (Fig. 2). Out of 30 crystals screened, six diffracted to better than 3 Å and a further eight crystals diffracted to better than 3.25 Å resolution.

A crystal of deglycosylated S1S2-B cryoprotected with MPD showed laboratory diffraction to 4 Å and yielded a full data set to 2.6 Å resolution at ESRF-ID14-2. A representative diffraction pattern is presented in Fig. 3. Although some splitting of the reflection spots was apparent, the data could be readily processed with the *XDS* package (Kabsch, 1988) and the crystal parameters are shown in Table 1. The full-length S1S2-B construct is likely to adopt a highly elongated shape in solution (Abele *et al.*, 1999). Such molecules frequently exhibit Matthews coefficients (Matthews, 1968) as high as 6–7 $Å^3\ Da^{-1}$ rather than the usual values of 2–3 $Å^3\ Da^{-1}$ (*e.g.* Rosenthal & Zhang, 1998). Taking the resolution limit and fragility of the crystals into account, it seems most likely that there are four molecules per asymmetric unit, yielding a calculated V_M of 4.6 $Å^3\ Da^{-1}$ and a solvent content of 73%. However, up to eight molecules may be present per asymmetric unit, which would yield V_M = 2.3 $Å^3\ Da^{-1}$ and a solvent content of 46%.

A self-rotation function calculated using the *REPLACE* programs (Tong, 1993) revealed a clear non-crystallographic

Table 1
Data-collection statistics.

Unit-cell parameters: a = 86.3, b = 85.6, c = 186.5 Å, β = 98.5°.

	Overall data	High-resolution shell
X-ray source and wavelength (Å)	ESRF-ID14-2 (0.933)	
Resolution range (Å)	30–2.6	2.7–2.6
Number of observations	178711	9112
Number of unique reflections	78228	5347
$R_{\rm merge}$† (%)	5.4	25.5
Completeness (%)	93.0	59.7
Multiplicity	2.3	1.7
$I/\sigma(I)$	11.6	2.5
N ($Z \leq 0.1$)‡	9.0	

† $R_{\rm merge} = (\sum|I - \langle I\rangle|)/(\sum I)$. ‡ Percentage of reflections with intensity $\leq 0.1 I_{\rm mean}$.

symmetry (NCS) twofold axis at 29–54% of the height of the crystallographic twofold axis, depending on the resolution range and Patterson sphere radius chosen. The NCS twofold axes are located in the *ac* plane offset ∼3° from the $\overline{a}$ and $\overline{a} \times \overline{c}$ directions, respectively, and most likely account for the pseudo-merohedral twinning observed in the absence of MPD treatment.

Locked cross-rotation function calculations performed using the S1S2 core/kainate complex structure (Armstrong *et al.*, 1998; Protein Data Bank entry 1eul) as a search model yielded several candidate orientations, depending on the resolution range and Patterson sphere radius selected. Patterson correlation refinement of the orientation of individual lobes of the protein resulted in very small adjustments (<1 Å translations and <0.5° rotations). However, translation-function searches have so far failed to yield obvious solutions, *e.g.* maximum correlation coefficients are less than 13% over the resolution range 10–4 Å. Some of the top solutions exhibit acceptable lattice packing and the low correlation coefficients may reflect the fact that even a monomer represents only 12.5–25% of the scattering mass of the asymmetric unit. In this case, it may be possible to bootstrap a molecular-replacement solution, adding successive monomers. Alternatively, the low correlation coefficients may reflect conformational differences between the apo- and kainate-bound states, in which case it is likely that a structure solution will require experimental phase determination. Both approaches are currently being pursued.

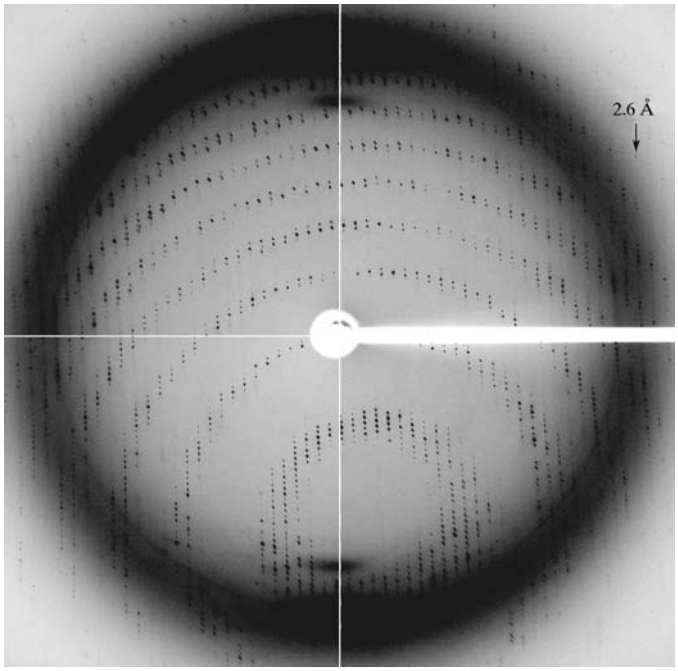

Figure 3
High-resolution diffraction pattern of deglycosylated S1S2-B flash-cooled with 10% MPD as cryoprotectant. Data were collected at ESRF beamline ID14-2 at 100 K with an oscillation range of 0.5° and an exposure time of 15 s.

We thank U. Reygers for skillful technical assistance and the Departments of Biophysics and Cell Physiology at the MPIMF for supporting this work. We thank the scientific staff at beamlines ID13 and ID14 (-1,2,3) (ESRF) and X11 (DESY) for help during data collections. Financial support was provided in part by EU grant BIO4-CT96-0589 of the Fourth Framework Program in Biotechnology (DRM and KK) and the Academy of Finland (KK).

References

Abele, R., Keinänen, K. & Madden, D. R. (2000). *J. Biol. Chem.* **275**, 21355–21363.
Abele, R., Svergun, D., Keinänen, K., Koch, M. H. J. & Madden, D. R. (1999). *Biochemistry*, **38**, 10949–10957.
Armstrong, N., Sun, Y., Chen, G.-Q. & Gouaux, E. (1998). *Nature (London)*, 395, 913–917.
Baker, H. M., Day, C. L., Norris, G. E. & Baker, E. N. (1994). *Acta Cryst.* D**50**, 380–384.
Brennan, P. A. (1994). *Neuroscience*, **60**, 701–708.
Collaborative Computational Project, Number 4 (1994). *Acta Cryst.* D**50**, 760–763.
Cramer, P., Bushnell, D. A., Fu, J., Gnatt, A. L., Maier-Davis, B., Thompson, N. E., Burgess, R. R., Edwards, A. M., David, P. R. & Kornberg, R. D. (2000). *Science*, **288**, 640–649.
Davidson, D. J. & Castellino, F. J. (1991). *Biochemistry*, **30**, 6167–6174.
Davidson, D. J., Fraser, M. J. & Castellino, F. J. (1990). *Biochemistry*, **29**, 5584–5590.
Davis, S. J., Puklavek, M. J., Ashford, D. A., Harlos, K., Jones, E. Y., Stuart, D. I. & Williams, A. F. (1993). *Protein Eng.* **6**, 229–232.
Dingledine, R., Borges, K., Bowie, D. & Traynelis, S. F. (1999). *Pharm. Rev.* **51**, 7–61.
French, G. S. & Wilson, K. S. (1978). *Acta Cryst.* A**34**, 517.
Grueninger-Leitch, F., D'Arcy, A., D'Arcy, B. & Chène, C. (1996). *Protein Sci.* **5**, 2617–2622.
Hollmann, M. & Heinemann, S. (1994). *Annu. Rev. Neurosci.* **17**, 31–108.
Hoover, D. M., Schalk-Hihi, C., Chou, C.-C., Menon, S., Wlodawer, A. & Zdanov, A. (1999). *Eur. J. Biochem.* **26**2, 134–141.
Jancarik, J. & Kim, S.-H.(1991). *J. Appl. Cryst.* **24**, 409–411.
Kabsch, W. (1988). *J. Appl. Cryst.* **21**, 916–924.
Keinänen, K., Kohr, G., Seeburg, P. H., Laukkanen, M.-L. & Oker-Blom, C. (1994). *Biotechnology*, **12**, 802–806.
Krupp, J. J., Vissel, B., Heinemann, S. F. & Westbrook, G. L. (1998). *Neuron*, **20**, 317–327.
Kulakosky, P. C., Hughes, P. R. & Wood, H. A. (1998). *Glycobiology*, **8**, 741–745.

Kuusinen, A., Arvola, M. & Keinänen, K. (1995). *EMBO J.* **14**, 6327–6332.
Madden, D. R., Abele, R., Andersson, A. & Keinänen, K. (2000). *Eur. J. Biochem.* **267**, 4281–4289.
Matthews, B. W. (1968). *J. Mol. Biol.* **33**, 491–497.
Mitchell, E. P. & Garman, E. F. (1994). *J. Appl. Cryst.* **27**, 1069–1074.
Nakanishi, H. & Masu, M. (1994). *Annu. Rev. Biophys. Biomol. Struct.* **23**, 319–348.
Nakanishi, H., Shnieder, N. A. & Axel, R. (1990). *Neuron*, **5**, 569–581.
Rees, D. C. (1980). *Acta Cryst.* A**36**, 578–581.
Rosenthal, P. B. & Zhang, X. (1998). *Nature (London)*, **396**, 92–96.
Schick, B. & Jurnak, F. (1994). *Acta Cryst.* D**50**, 563–568.
Sommer, B., Keinänen, K., Verdoorn, T. A., Wisden, W., Burnashev, N., Herb, A., Köhler, M., Takagi, T., Sakmann, B. & Seeburg, P. H. (1990). *Science*, **249**, 1580–1585.
Stern-Bach, Y., Bettler, B., Hartley, M., Sheppard, P. O., O'Hara, P. J. & Heinemann, S. F. (1994). *Neuron*, **13**, 1345–1357.
Tong, L. (1993). *J. Appl. Cryst.* **26**, 748–751.
Villarroel, A., Paz-Regalado, M. & Lerma, J. (1998). *Neuron*, **20**, 329–339.
Wyss, D. F. & Wagner, G. (1996). *Curr. Opin. Biotechnol.* **7**, 409–416.
Yeates, T. O. & Fam, B. C. (1999). *Structure*, **7**, 25–29.